Science Advances
AAAS

Supplementary Materials for

High-fat feeding drives the intestinal production and assembly of $C_{16:0}$ ceramides in chylomicrons

Michael SM Mah *et al.*

Corresponding author: Sarah M. Turpin-Nolan, Sarah.Turpin-Nolan@monash.edu;
Mark A. Febbraio, Mark.Febbraio@monash.edu

Sci. Adv. **10**, eadp2254 (2024)
DOI: 10.1126/sciadv.adp2254

This PDF file includes:

Figure S1. related to figure 2 and 3

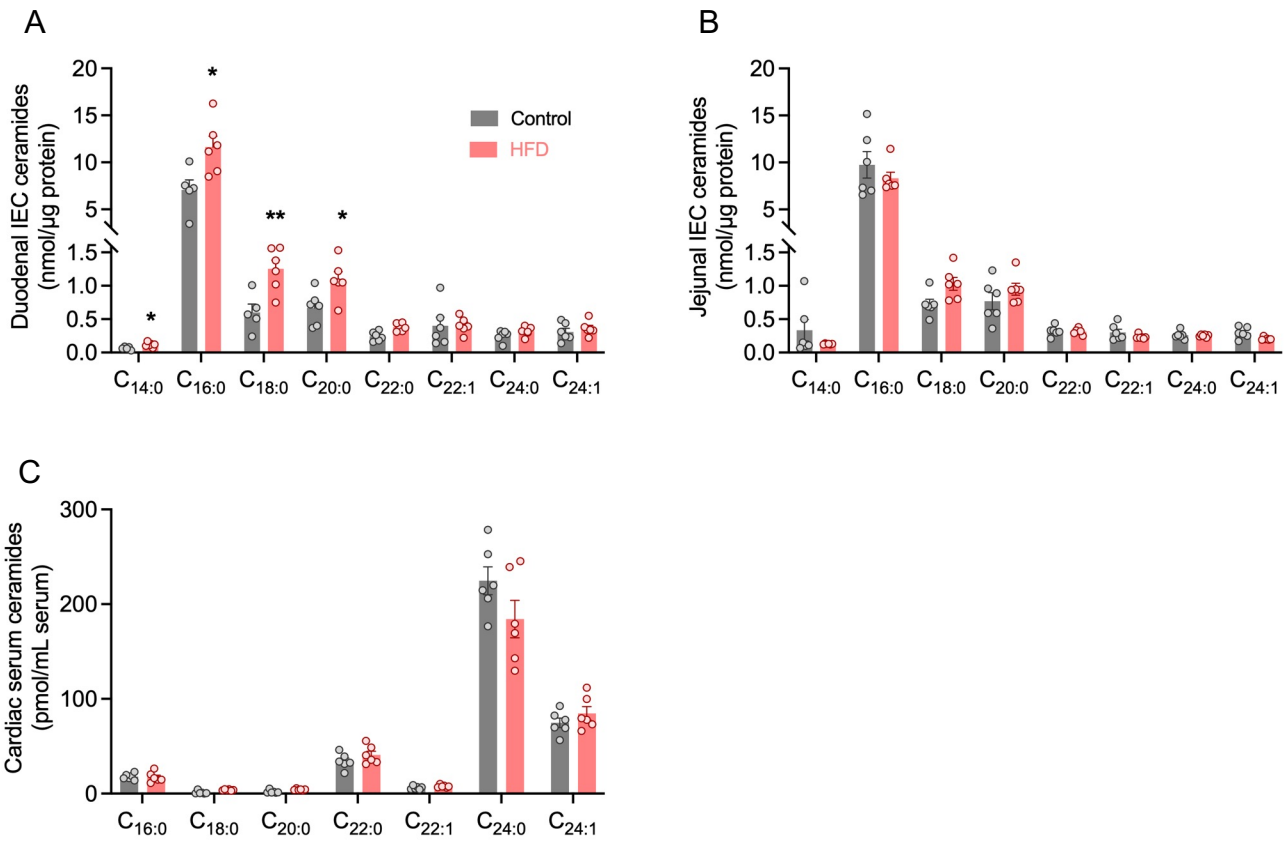

Figure S1. **Sham rat gut and systemic ceramide profiles are comparable to ceramide profiles from rats undergoing lymph cannulation.** Lipidomic quantitation of individual ceramides in (A) duodenal, (B) jejunal epithelial cells and (C) cardiac serum from rats fed either a control or high-fat diet (n=6/group). Data are expressed as means ± SEM. **P* < 0.05, ***P* < 0.01.

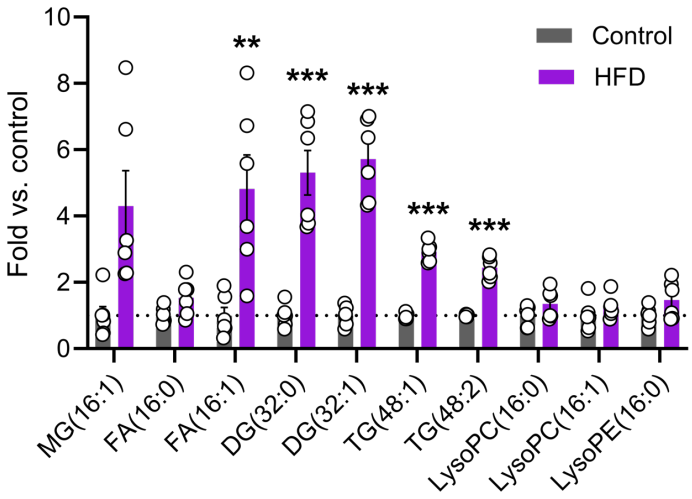

Figure S2. **High-fat feeding amplifies $C_{16:0}$ fatty acid processing of multiple lipid species in mesenteric lymph-derived chylomicrons**. Untargeted lipidomic quantitation of lipids containing a $C_{16:0}$ fatty acid chain in chylomicron from control and high-fat diet-fed rats (n=6/group). Data are expressed as means ± SEM. $^{**}P < 0.01$, $^{***}P < 0.001$.

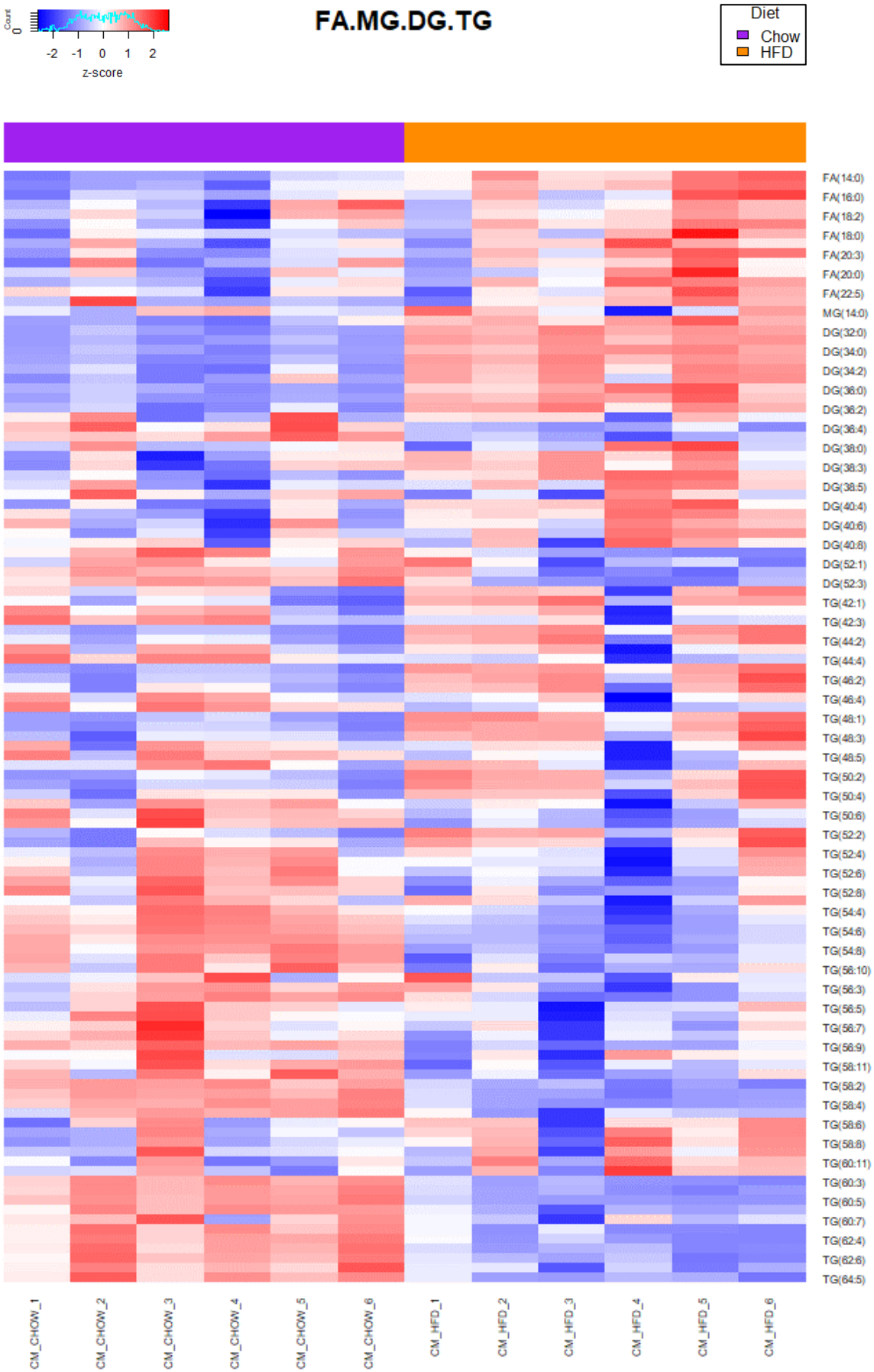

Figure S3. **High-fat feeding alters the chylomicron lipidome**. Untargeted, semi-quantitative, lipidomic data clustering of mesenteric lymph-derived chylomicrons from control and high-fat diet-fed rats. Hierarchical clustering analysis (heat map) of lipid analytes from the following classes: fatty acyls, monoacylglycerols, diacylglycerols, and triacylglycerols.

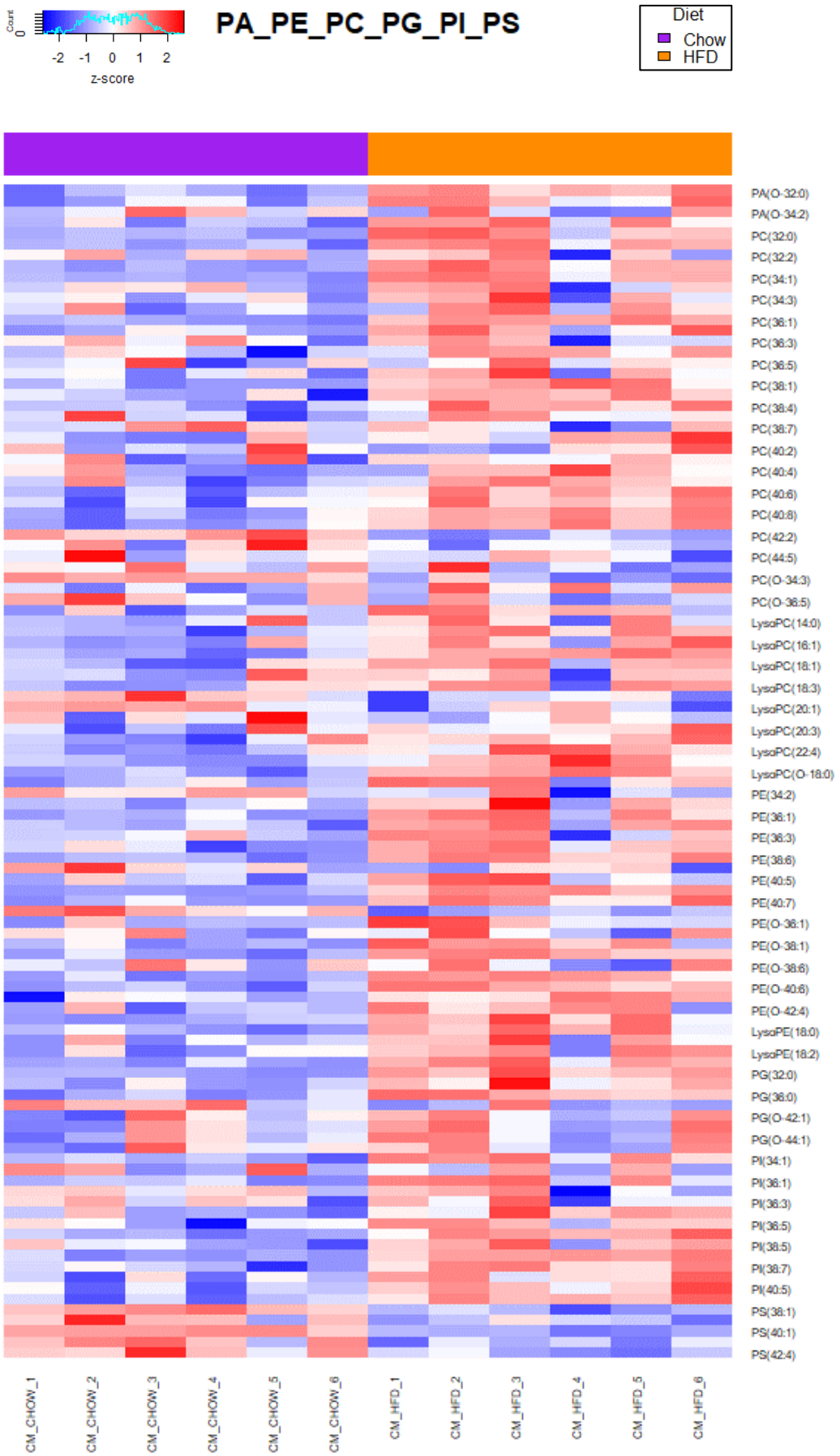

Figure S4. **High-fat feeding alters the chylomicron lipidome**. Untargeted, semi-quantitative, lipidomic data clustering of mesenteric lymph-derived chylomicrons from control and high-fat diet-fed rats. Hierarchical clustering analysis (heat map) of lipid analytes from the following classes: phosphates (PA), phosphocholines (PC), phosphoethanolamines (PE), phosphoglycerols (PG), phosphoinositols (PI), and phosphoserines (PS).

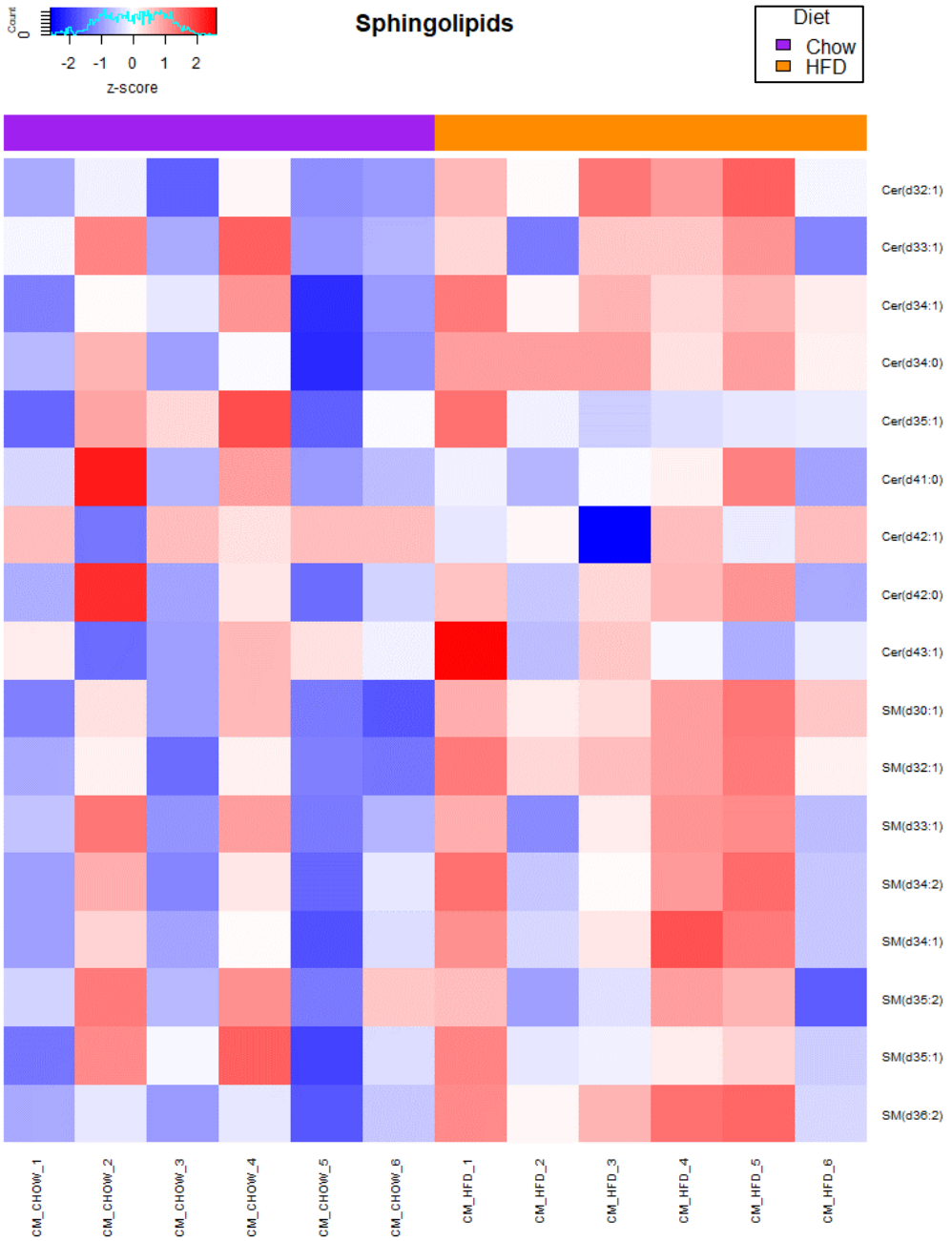

Figure S5. **High-fat feeding alters the chylomicron lipidome**. Untargeted, semi-quantitative, lipidomic data clustering of mesenteric lymph-derived chylomicrons from control and high-fat diet-fed rats. Hierarchical clustering analysis (heat map) of lipid analytes from the following classes: sphingolipids.

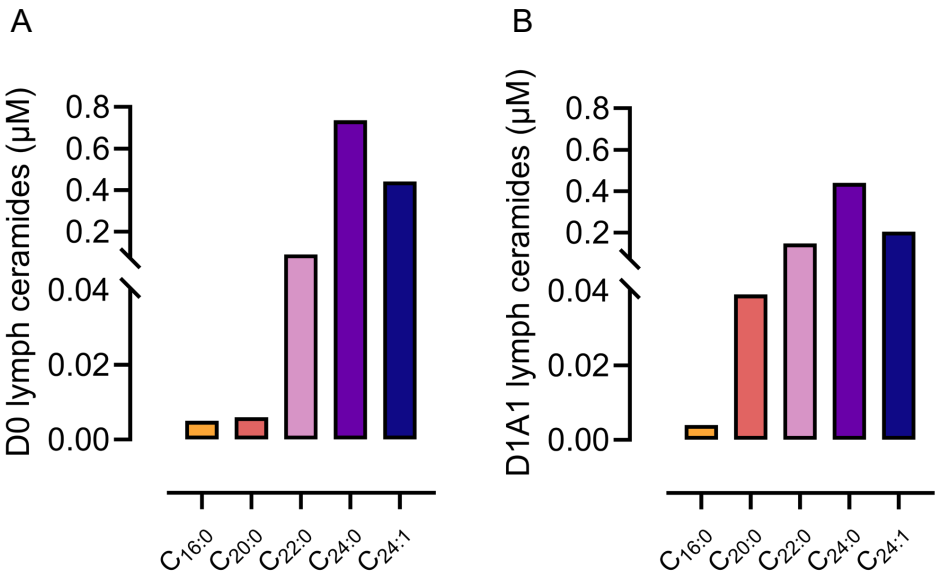

Figure S6. Comparison of two pre-lipid infusion timepoints reveal slight differences in ceramide accumulation in human thoracic lymph. Human thoracic lymph $C_{16:0}$, $C_{20:0}$, $C_{22:0}$, $C_{24:0}$ and $C_{24:1}$ ceramide levels at D0 and D1A1 timepoints captured prior to enteral lipid infusion in one patient.

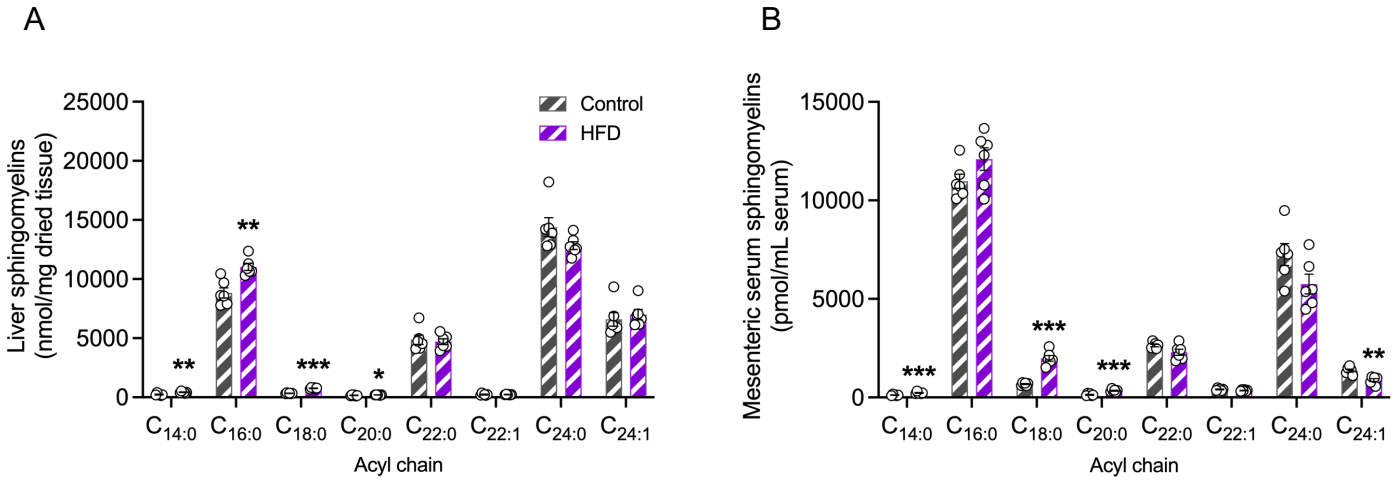

Figure S7. Hepatic and mesenteric serum sphingomyelin levels.
Lipidomic quantitation of individual sphingomyelins in (A) liver and (B) mesenteric serum from rats fed either a control or high fat diet (HFD). The following numbers of biological replicates were used (independent rats) per diet group in each experiment: n=6. Data are expressed as means ± SEM. *P < 0.05, **P < 0.01, ***P < 0.001.

Table S1

Human thoracic lymph DG and TG (μM)

	Lipid dose (mL/hr)		
DG/TG species	0	20	80
DG(32:1)	3.55	2.74	1.71
DG(32:2)	1.44	1.18	0.651
DG(34:1)	12.8	8.2	11.1
DG(34:3)	1.74	1.22	1.5
DG(36:2)	12.3	18.9	37.8
DG(36:3)	10.4	12.5	21.3
DG(36:4)	3.66	5.16	8.93
DG(38:0)			
DG(38:5)	1.4	0.662	0.61
DG(39:0)	0.722	0.514	0.246
DG(41:1)	0.391	0.245	0.18
DG(42:0)	0.002	0.003	0.004
DG(42:1)	0.003	0.119	0.094
DG(42:2)	0.063	0.298	0.19
DG(44:3)		0.28	0.619
DG-O(32:2)	0.975	3.84	5.48
DG-O(34:1)	5.66	50.5	143
DG-O(36:4)	0.544	1.08	3.99
TG(44:1)	8.55	66.2	73.2
TG(44:2)	3.76	112	224
TG(44:4)	0.208	29.4	56.2
TG(46:2)	6.81	145	249
TG(48:1)	23.3	39.6	7.13
TG(48:2)	15.2	37	17.8
TG(48:3)	4.18	15.6	8.46
TG(49:1)	3.74	6.11	1.75
TG(49:2)	2.34	4.08	2.21
TG(50:1)	54.4	54.7	36.1
TG(50:2)	53	78.8	64.7
TG(50:3)	19.7	37.3	30.7
TG(50:4)	6.97	15.4	13.9
TG(51:1)	3.05	2.66	1.43
TG(51:2)	5.58	9	7.85
TG(51:3)	2.86	5.36	5.79
TG(51:4)	0.88	2.04	2.37
TG(51:5)	0.3	1.01	0.923
TG(52:2)	119	160	336
TG(52:3)	102	166	238
TG(52:4)	36	74.8	115
TG(52:5)	7.33	20.9	32.4

TG(52:6)	1.93	7.02	10.8
TG(52:7)	0.041	2.83	3.73
TG(53:3)	3.45	5.3	7.27
TG(53:4)	1.6	2.96	4.28
TG(53:5)	0.682	1.69	2.02
TG(53:6)	0.228	1.07	0.994
TG(54:2)	7.99	0.03	0.064
TG(54:3)	39.8	80	156
TG(54:4)	33.4	276	663
TG(54:5)	18.4	157	340
TG(54:6)	9.7	60.3	119
TG(54:7)	2.75	16.9	33
TG(55:6)	0.581	1.01	1.17
TG(55:7)	0.394	0.62	1.07
TG(55:8)	0.01	0.213	0.49
TG(55:9)	0.007	0.18	0.194
TG(56:6)	7	9.19	10.9
TG(56:7)	8.83	19	32.5
TG(56:8)	3.81	9.67	14.8
TG(56:9)	0.459	2.36	4.42

Human thoracic lymph sphingolipids (μM)

	Lipid dose (mL/hr)		
Ceramide species	0	20	80
C16:0	0.004	0.025	0.104
C20:0	0.039	0.01	0.031
C22:0	0.147	0.042	0.097
C24:0	0.44	0.364	0.407
C24:1	0.204	0.27	0.235
Sphingomyelin species			
C14:0	2.86	2.41	2.51
C16:0	38.8	32.5	31.7
C18:0	7.4	6.8	4.55
C20:0	4.12	3.65	
C22:0	6.43	4.58	0.013
C22:1	5.94	5.42	4.83
C24:0	4.01	2.64	2.96
C24:1	11.3	8.6	7.23

Table S2. Human thoracic lymph sphingolipids (μM) during increasing rates of enteral lipid infusion.

	Lipid dose (mL/hr)		
	0	**20**	**80**
Ceramide species (μM)			
C16:0	0.004	0.025	0.104
C20:0	0.039	0.01	0.031
C22:0	0.147	0.042	0.097
C24:0	0.44	0.364	0.407
C24:1	0.204	0.27	0.235
Sphingomyelin species (μM)			
C14:0	2.86	2.41	2.51
C16:0	38.8	32.5	31.7
C18:0	7.4	6.8	4.55
C20:0	4.12	3.65	
C22:0	6.43	4.58	0.013
C22:1	5.94	5.42	4.83
C24:0	4.01	2.64	2.96
C24:1	11.3	8.6	7.23